

Statistical analysis of the indentation rolling resistance measurement according to DIN EN 16 974 for the validation of simulation models

Statistische Betrachtung der Eindrückrollwiderstandsmessung nach DIN EN 16 974 zur Validierung von Simulationsmodellen

Malte Kanus
Carsten Schmidt
Ludger Overmeyer

Institute of Transport and Automation Technology
Leibniz University Hannover

The most significant challenges in belt conveyor technology are continuously increasing mass flows and conveying distances. The resulting increase in movement resistance is thus responsible for the necessary increase in drive power. For the design of belt conveyor systems, it is essential to gain knowledge of the movement resistances that occur. The main resistance comprises indentation rolling resistance (IRR), idler running resistance, vibration bending resistance, bulk material rolling resistance, and camber resistance. The IRR represents the most significant component of the movement resistance for horizontal belt conveyors. Due to the resulting particular importance for the design of belt conveyor systems, a test method for determining the IRR was developed at Institute of Transport and Automation Technology (ITA) and standardized in DIN EN 16 974. This established measurement method is costly and time-consuming, which is why investigations are being carried out at ITA to determine the ERW by simulation. The material parameters required for the simulation are determined from small samples, which support the development of energy-optimized conveyor belts and make them more efficient. The validation of the simulation results bases on the previous metrological determination. Therefore, the statistical proof of the established measurement procedure is of particular interest.

[Keywords: Indentation rolling resistance (IRR), belt conveyor systems, Energy optimization, CO₂ reduction, DIN22101, DIN EN 16 974]

Die größten Herausforderungen in der Gurtfördertechnik stellen kontinuierlich steigende Massenströme sowie Förderstrecken dar. Die hieraus resultierende Erhöhung der Bewegungswiderstände ist somit für eine notwendige Steigerung der Antriebsleistung verantwortlich. Für die Auslegung von Gurtförderanlagen ist es deshalb von besonderer Wichtigkeit, Kenntnis über die sich einstellenden Bewegungswiderstände zu erlangen.

Der Hauptwiderstand setzt sich aus Eindrückrollwiderstand (ERW), Tragrollenlaufwiderstand, Schwingbiegewiderstand, Schüttgutwalkwiderstand und Sturzwiderstand zusammen. Der stellt ERW den größten Bestandteil des Bewegungswiderstandes für horizontale Gurtförderanlagen dar. Aufgrund der daraus resultierenden besonderen Wichtigkeit für die Auslegung von Gurtförderanlagen wurde am Institut für Transport- und Automatisierungstechnik (ITA) ein Prüfverfahren zur Ermittlung des ERW entwickelt und in DIN EN 16 974 genormt. Dieses etablierte Messverfahren ist kosten- und zeitaufwendig, weshalb am ITA Untersuchungen zur simulativen Bestimmung des ERW durchgeführt werden. Die hierfür notwendigen Materialparameter werden aus kleinen Proben ermittelt, wodurch die Entwicklung energieoptimierter Fördergurte unterstützt und effizienter gestaltet wird. Die Validierung der Simulationsergebnisse basiert auf die bisherige messtechnische Ermittlung. Deshalb ist die statistische Absicherung des etablierten Messverfahrens von besonderem Interesse.

[Schlüsselwörter: Eindrückrollwiderstand (ERW), Gurtförderanlagen, Energieoptimierung, CO₂ Reduzierung, DIN 22101, DIN EN 16 974]

1 INTRODUCTION

Belt conveyors are continuous mechanical conveyors which use an endless conveyor belt as a supporting element. With the help of this belt, bulk materials or unit loads can be conveyed continuously, in cycles, or at varying speeds from a feed point to one or more discharge points. The belt supports the bulk material and acts as a traction element required for the movement. It is tensioned around two drums in the simplest case, one serving as the drive drum and the other as the tensioning drum.

Figure 1 shows the schematic structure and the resulting resistances of such a belt conveyor system with the essential components. Bulk material and the belt itself generate large loads, while support idlers stabilize the so-called upper run and lower run. They reduce the belt sagging and thus the movement resistance.

Additional impact plates are used to protect the belt, particularly when handling goods from a great height or when emptying a silo. As a result, however, the movement resistance in the area of the feed increases again.

Since a reduction of the conveying speed due to decreasing mass flows and efficiency losses is usually not desired by plant operators, the following article focuses on the most crucial component of the motion resistance. In the case of horizontally running systems, this is the indentation rolling resistance (IRR), which accounts for 62 % of the total amount (cf. Figure 2) which can be confirmed by VON DAAKE [DAA18]. [WEN08]

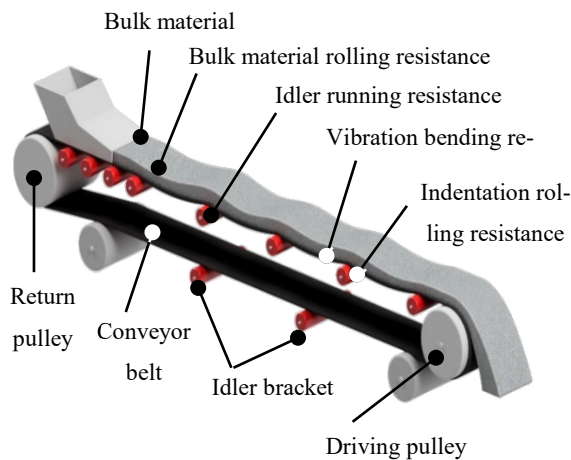


Figure 1. Structure of a belt conveyor system and points of origin of the movement resistances

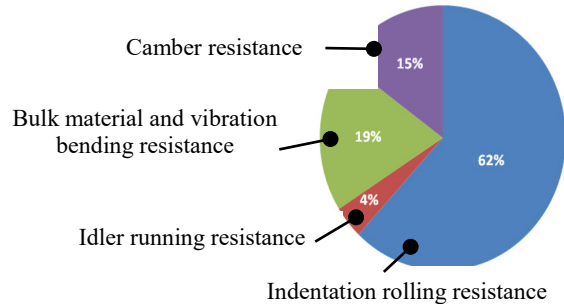


Figure 2. Division of the individual resistances of a horizontally running belt conveyor system according to [WEN08]

2 RESISTANCES ON CONVEYOR BELT SYSTEMS

For constant mass flow, belt conveyors are driven by electric motors. As shown in eq. 1, the drive power P required for this is composed of conveying speed v and the resistance to movement F_W occurring along with the entire conveying distance.

$$P = F_W \cdot v \quad 1$$

The system's design predetermines the movement resistances occurring on belt conveyors and are therefore difficult to modify after commissioning. The dominant factors here are the conveying length L , the belt angle δ to be overcome, and specially used peripheral parts such as belt scrapers or sealing strips (depending on the upper or lower run).

According to eq. 2, the total resistance to motion F_W is the sum of the main resistance F_H , the secondary resistance F_N , the inclination resistance F_{St} , and the special resistance F_S :

$$F_W = F_H + F_N + F_{St} + F_S \quad 2$$

Within the scope of this article, the general procedure for system design according to DIN 22101 [DIN11], which considers a stationary operating condition, is used to explain the individual resistances. This idealized approach ignores negative influences, such as those that occur when the system is started up and calculates all resistances based on a constant material flow.

Hereby, the structure visualized in Figure 1 serves as an example conveyor to illustrate the individual resistances and their determination.

The friction resistances occurring in the system are described as most significant portion of the total movement resistances. With aid of the main resistance, assuming a linear relationship between moving loads and friction, they are taken into consideration. These include the running resistance of the idlers, the frictional resistance between the belt and the sliding plates used, the resistance to oscillating bending and load rolling of the belt in the case of slack, and the rolling resistance to indentation between the idlers and the running side of the belt.

The further investigation of the IRR has excellent potential for reducing drive power, due to its major part of the main resistance. Depending on the technical realization of the upper and lower run, the main resistance F_H is composed of locally occurring the partial resistances ($F_{H,o}$ for the upper run and $F_{H,u}$ for the lower run).

$$F_H = F_{H,o} + F_{H,u} \quad 3$$

The reason for the separate consideration of the individual run sections is a different idler distribution. Due to the additional bulk material weight, the idler spacing in the

upper run must be much smaller than is necessary when returning the empty lower run. The respective partial resistance in the upper run $F_{H,o}$ and the lower run $F_{H,u}$ can be determined according to [DIN11] as in eq. 4 and eq. 5 which components are described in the following:

$$F_{H,o} = L \cdot f_f \cdot g \cdot [m_{R,i}' + (m_G' + m_L') \cdot \cos(\delta)] \quad 4$$

$$F_{H,u} = L \cdot f_f \cdot g \cdot [m_{R,i}' + m_G' \cdot \cos(\delta)]. \quad 5$$

A fictitious friction value f_f is used to simulate the inertia resistance of the idlers, the indentation rolling resistance and the fulling resistance of the tension members as a function of ambient temperature and conveying speed [VIE60]. [DIN11] delivers guide values.

The required width related line load of the idlers $m_{R,i}'$ is composed of their number n_i , their roller weight $m_{R,i}$, and the roller spacing used $l_{R,i}$.

$$m_{R,i}' = \frac{n_i \cdot m_{R,i}}{l_{R,i}} \quad 6$$

To calculate the width related line load of the belt m_G' (see eq. 7), the installed belt width B and the specific weight per unit area of the belt m_{Gk} are necessary.

$$m_G' = B \cdot m_{Gk} \quad 7$$

The bulk material to be transported in the upper run results in the width related line load m_L' for the same run section as shown in eq. 8.

$$m_L' = A \cdot \rho \quad 8$$

The filling cross section A , which depends on the trough shape and specific properties of the bulk material, such as its density ρ , is of great importance.

Locally occurring individual resistances, mainly frictional and inertial forces, are summarized in the secondary resistance of a belt conveyor. Typical examples are losses at tensioning, drive, and deflection pulleys and resistances induced by material tasks and belt cleaners.

If considering conveyor lengths of $L > 80$ m, eq. 9 [DIN11, p. 20] provides a general determination. Here, an experimentally determined length coefficient C is used. However, for shorter conveyors, the deviations are too large, requiring an exact calculation in these cases.

$$F_N = (C - 1) \cdot F_H \quad 9$$

If the conveying distance is not purely horizontal but has one or more height differences h , lifting work must be performed for upward conveying. So the lifting work harms the inclination resistance. In contrast, the effect is

positive in the case of downward conveyance due to generative operation.

With the stroke to be overcome (eq. 10), the inclination resistance follows from eq. 11.

$$h = L \cdot \sin(\delta) \quad 10$$

$$F_{St} = h \cdot g \cdot m_L' \quad 11$$

The special resistance mentioned in eq. 2 can occur in the form of additional frictional resistance when using special internals.

3 ORIGIN OF THE INDENTATION ROLLING RESISTANCE

As explained above, idlers stabilize the conveyor belt. Its own weight and the bulk material causes deformations in the contact area between the idler and the belt. This produces a resistance opposite to the conveying movement, the so-called indentation rolling resistance F_{IR} .

Figure 3 shows a schematic contact situation between idler and belt. The deformation is divided into a compression occurring during run-up and a visible stretching back of the rubber, while running-off. WENNEKAMP [WEN08] states that both the compression and the recovery are time-delayed due to the rheological material behavior of elastomers.

One possibility for the experimental determination of the indentation rolling resistance is the test method according to DIN EN 16974 [DIN16], which bases on [WEN08].

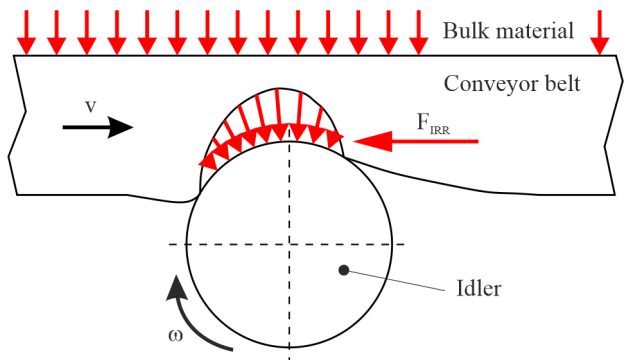


Figure 3. Contact situation between idler and belt according to [WEN08]

A more detailed overview of the force ratio occurring at idlers is provided by Figure 4, which shows a symmetrical arc of contact between the belt and idler at rest (Figure 4, left). The vertical force F_V generated by the bulk material and belt weight transmits into the steel structure of the system in the form of reaction force \bar{F}_V via the idler.

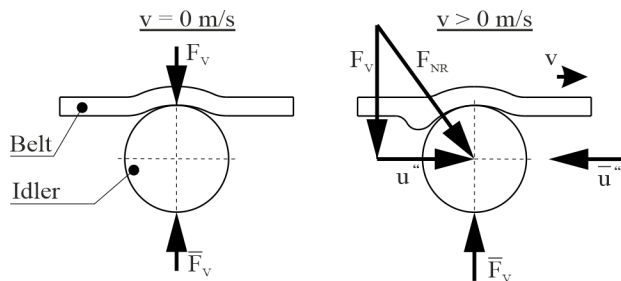


Figure 4. Force ratios on idlers according to [GEE01]

As result of a conveying movement (Figure 4, right), the deformation mentioned above occurs when the belt runs up. The bulk material and belt weight generates the oblique normal force F_{NR} composed of the weight-induced vertical force F_V and the horizontally acting flexing resistance u'' . In this case, its reaction force \bar{u}'' , opposite the conveying direction, is equal to the indentation rolling resistance F_{IRR} .

According to KÖNIG [KÖN03], both compressive and shear stresses occur in the contact area in addition to the force ratio. The Hertzian Contact provides two elastic bodies, which generates the compressive stress curve shown in Figure 5 (blue). Here, the greatest stress occurs in the center of the idler (by definition, an angle of 0°). Due to the geometry-related idler curvature, the shear stresses visualized in Figure 5 (red) also occur. If there is Coulomb friction between the belt and idler, the belt velocity v corresponds approximately to the tangential idler circumferential velocity v_R but is not identical. The reason for this is the previously explained deformation of the rubber on the running side. Due to locally different moduli of elasticity, the maximum shear stresses occur in the run-up and run-off areas of the idler.

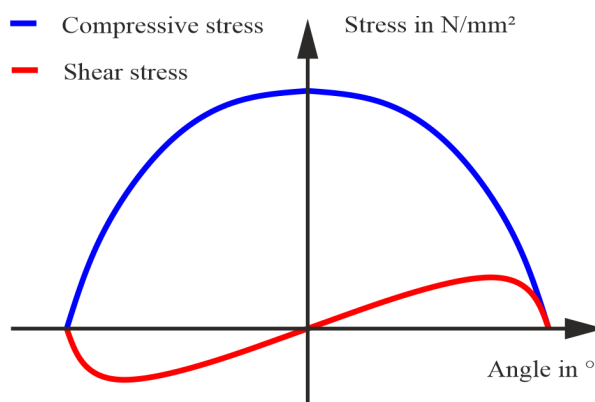


Figure 5. Stress curve on idlers according to [KÖN03]

The two velocities are identical $v = v_R$ in the roller core (angle 0°), whereby the shear stresses drop to 0 N/mm^2 . In general, occurring shear stresses are much lower than the compressive stresses, which means that they have no appreciable influence concerning the indentation rolling resistance and are only relevant for determining the slip.

Further influences on the indentation rolling resistance could be verified thanks to experimental investigations and are currently used to develop new conveyor belts. For example, HINTZ mentions that the IRR also decreases with decreasing barrel side thicknesses, which leads to a smaller material volume and results in more minor deformations between the idler and the belt. Increasing the carbon content within the rubber compound realizes the same behavior. With decreasing temperatures, however, the indentation rolling resistance increases due to greater material stiffness. [HIN93]

As SCHWARZ illustrates, the selected process parameters also significantly influence the indentation rolling resistance. The effect is most significant with the selection of the idler diameter. With increasing diameter, the indentation rolling resistance decreases hyperbolically, thus providing a good adjustment variable already in the design phase. On the other hand, increasing vertical loads due to larger filling ratios and higher tensile strengths of the conveyor belt provide a progressive increase in the indentation rolling resistance. Increasing conveying speed has the effect of a degressive increase. [SCH66]

The high significance of the indentation rolling resistance on the energy requirement regarding the design and operation of conveyor belt systems, mainly due to the increasing pressure for CO₂ reduction, places the development of energetic optimized conveyor belts in the center of attention.

4 EXPERIMENTAL PERFORMANCE AND MEASUREMENT DATA ANALYSIS

As shown above, the indentation rolling resistance depends on various parameters. In order to gain quantitative information about the IRR, a test rig was developed at ITA [HIN93] and improved on this basis [SCH04, WEN08]. The measurement method was further developed and initially standardized in DIN 22123 before being adopted throughout Europe in DIN EN 16974. The measurement setup for determining the indentation rolling resistance at the ITA is shown schematically in Figure 6.

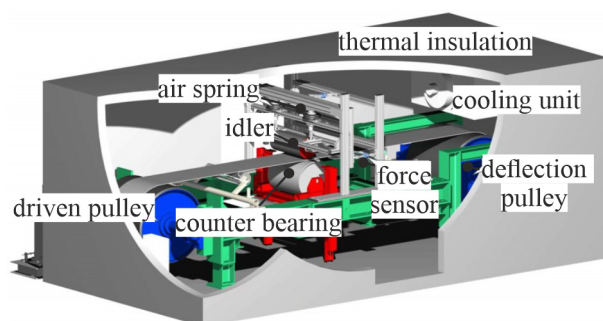


Figure 6. Setup of the measuring system for determining the indentation rolling resistance

The test rig for determining the indentation rolling resistance is set up as follows. The belt moves at an adjustable speed via a driving pulley and a deflection pulley comparable to a conveyor belt system. In the process, it passes through the measuring idler. Two air spring systems introduce adjustable forces into the measuring idler, whereby a counter bearing with a significantly larger diameter counteracts the load. The rotating belt, which deforms on the measuring idler, as shown in Figure 3, causes the indentation rolling resistance. Two force sensors measure the force on the idler. The whole test rig is thermally insulated for adjusting the temperature with a cooling and heating unit.

The belt speed and the idler diameter are investigated as influencing factors. The test requires a belt for each belt structure and elastomer compound, making the determination of the IRR very expensive. Added to this is the time-consuming testing of the individual parameter combinations. Figure 7 shows the results by way of example. For each load from 5 kN/m to 20 kN/m, the curves show its common dependency for temperature.

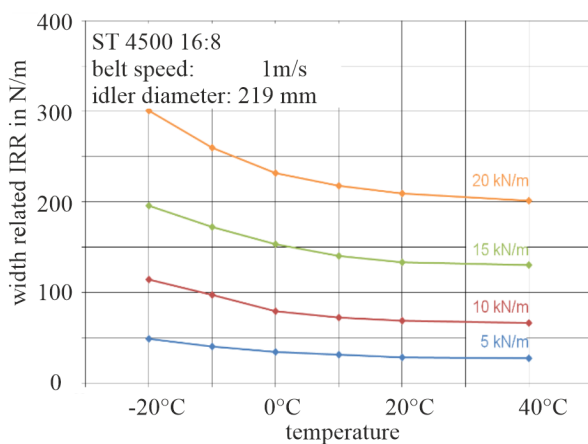


Figure 7. Example measurement results at different temperatures and superimposed loads

In order to eliminate directional dependencies of the system and the belt, a measurement procedure consists of six sections in which the belt running direction changes. Each of these sections has a recording time of 100 seconds, evaluating 40 seconds with a recording frequency of 200 Hz. Figure 8 shows a measurement. A strong scattering of the measured values can be seen. The figure shows the transitions between changes in running direction. The belt brakes and accelerates again. Only after a waiting time of approximately sixty seconds a steady-state is achieved again for all belt speeds. At low speeds, as in this measurement, the condition settles after only a short waiting time. However, a constant cycle is necessary for automated evaluation. The extended measurement cycle intends to provide statistically validated measurement results. The statistical consideration of the results is examined in more detail in this paper in more detail in this paper. The total time of a test cycle for a parameter combination thus lasts 600 seconds and rep-

resents a point in the curve array. The various test parameters of load and temperature changes create a curve array, as shown in Figure 7. This procedure must be repeated for each belt speed and idler diameter.

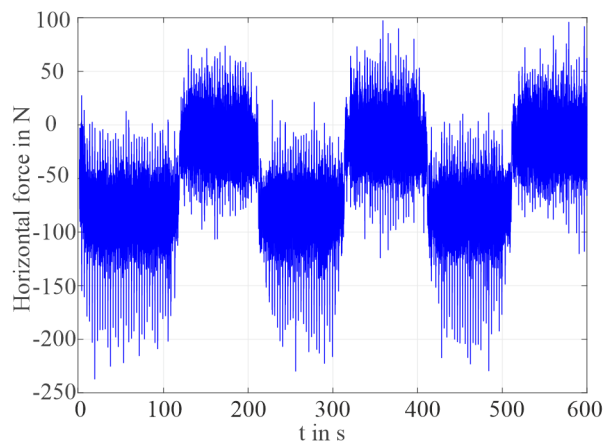


Figure 8. Measurement of the indentation rolling resistance for an exemplary parameter combination

To determine the indentation rolling resistance from these data sets, the transitions from the changes in running direction are removed, as the measured values generated during the passage of the belt splice. Due to their geometric deviations, there is a significantly increased scatter of the measured values, which would lead to inaccurate results. Figure 9 shows the adjusted measured values. Compared to Figure 8, these smaller deflections of horizontal forces are visible.

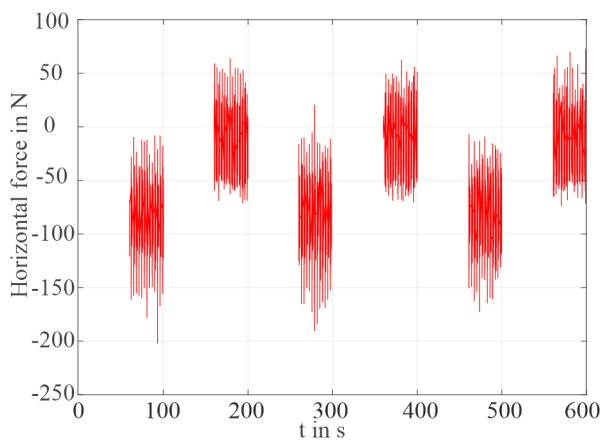


Figure 9. Adjusted measurement of the indentation rolling resistance for an exemplary parameter combination

For further evaluation, the mean values of the horizontal forces \bar{H}_k are calculated for each section. In addition, the standard deviation S_k is determined for each section k overall measured values of the section.

$$\bar{H}_k = \frac{1}{n} \sum_{k=1}^n H_k \quad 12$$

$$S_k = \sqrt{\frac{1}{n-1} \sum_{j=1}^n (x_{j,k} - \bar{H}_k)^2} \quad 13$$

Table 1 shows the calculated absolute mean values of the horizontal forces \bar{H}_k and table 2 the corresponding standard deviation S_k of each section. The standard deviation for the single confidence interval is between 18.5 N and 20.4 N. Thus, is relatively large considering the absolute measured values. However, the mean values in table 1 of sections one, three, and five and two, four, and six each show a slight deviation. Despite the high standard deviation of the individual measured values, this already suggests good repeatability. This assumption will be considered in more detail for further evaluation.

Figure 10 shows the histograms of each horizontal force H_k . Additionally it shows the normal distributions calculated with the corresponding mean value \bar{H}_k and standard deviation S_k . This illustrates the normally distributed

measured values and confirms the evaluation procedure for mean values.

Table 1. Absolute mean values of horizontal forces \bar{H}_1 to \bar{H}_6 for corresponding measuring sections

\bar{H}_1	\bar{H}_2	\bar{H}_3	\bar{H}_4	\bar{H}_5	\bar{H}_6
84.4 N	14.6 N	83.4 N	14.7 N	82.5 N	14.0 N

Table 2. Standard deviations of horizontal forces H_1 to H_6 for corresponding measuring sections

S_1	S_2	S_3	S_4	S_5	S_6
19.3 N	18.4 N	20.4 N	19.2 N	19.5 N	18.5 N

Figure 11 summarizes the normal distributions from figure 10 and the mean value of the right and left runs of the belt. It shows a high degree of correlation of corresponding measurements. The mean value of the right runs \bar{H}_{135} is -83.4 N and the mean value of the left runs \bar{H}_{246} is -14.4 N.

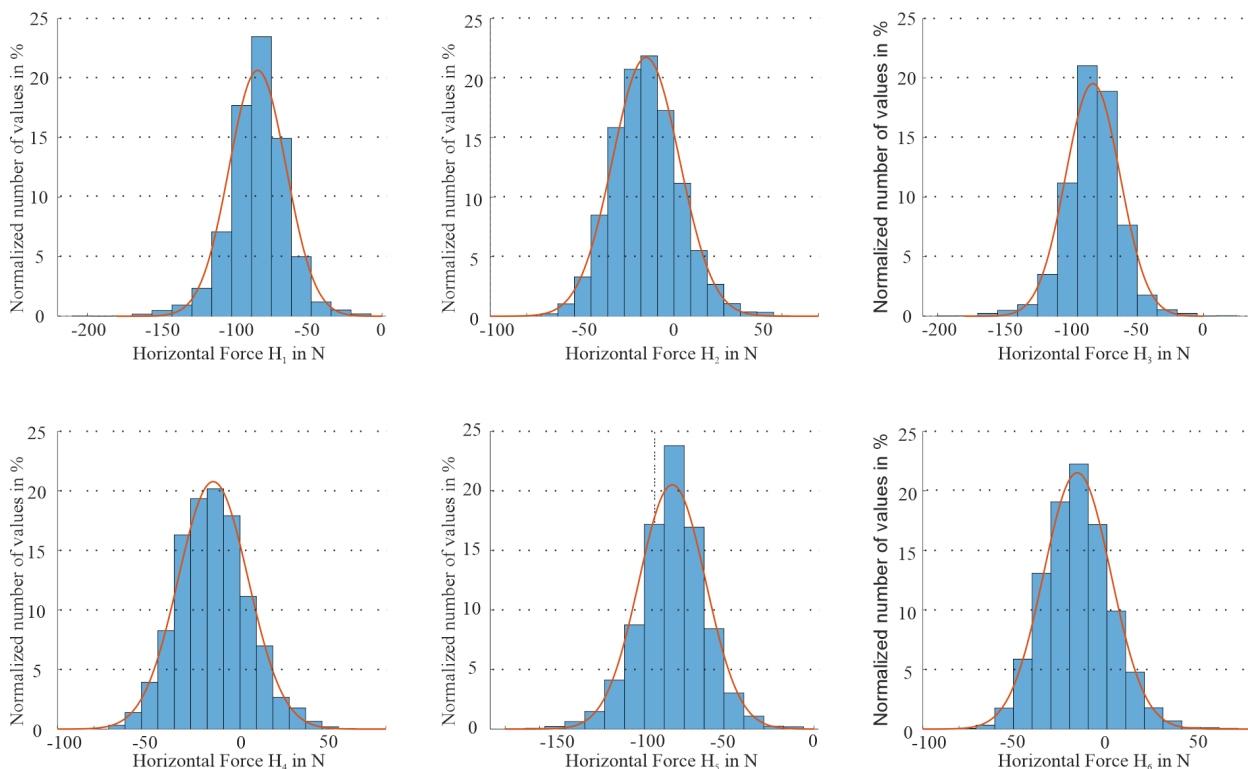


Figure 10. Histograms of horizontal forces H_1 (top left) to H_6 (bottom right) and corresponding normal distributions

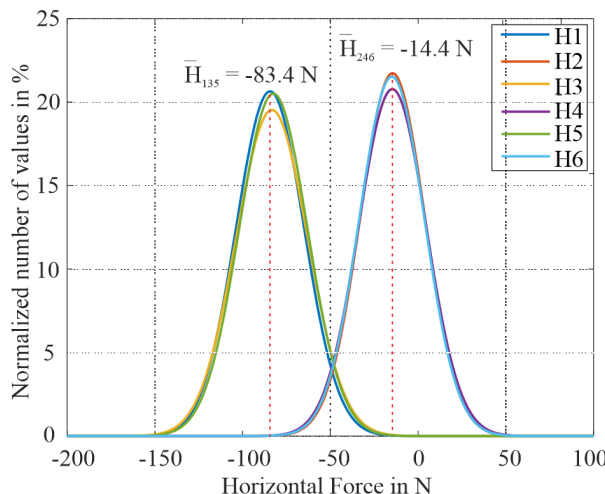


Figure 11. Summarized normal distributions of horizontal forces H_1 to H_6 and mean values of right and left runs

Figure 12 shows the average values of the forces acting horizontally on the idler, calculated section by section corresponding to table 1. Suppose the standard deviation for right and left running is considered separately. In that case, the results are 0.2 N and 0.9 N. The fact that there is a similarly slight deviation between the mean values can be observed over four series of 24 measurements each explicitly examined for this purpose at the ITA, confirming previously postulated repeatability.

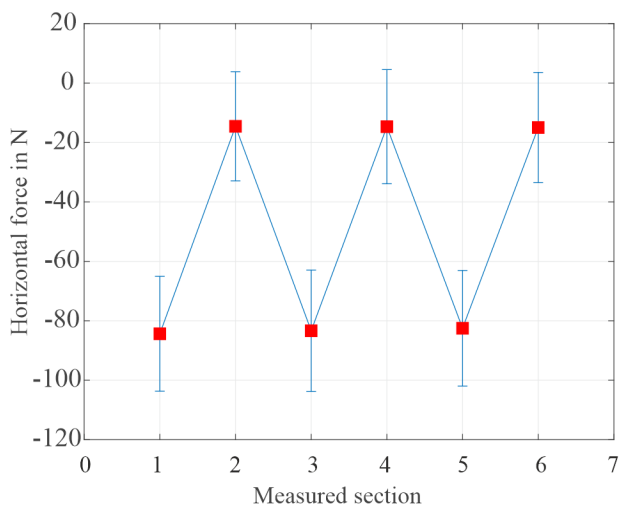


Figure 12. Section-by-section mean values of the horizontal force with an associated standard deviation

Calculating the indentation rolling resistance from the determined horizontal forces, the difference of successive right and left runs is shown in eq. 14.

$$\Delta H_i = |H_k - H_{k+1}| \quad 14$$

The results are presented below in table 3. The maximum difference ΔH_1 is 69.8 N. The minimum ΔH_6 is

67.6 N, thus having a deviation of $\Delta H = 2.3$ N. If the standard deviation is considered, there is a value of 0.9 N to the mean value of 68.5 N, representing the absolute indentation rolling resistance of the test belt. For the uniform presentation and better comparison, the indentation rolling resistance determined in this way is standardized to the belt width. The width-related indentation rolling resistance for the selected temperature and load is thus 171.3 N/m.

Table 3. Absolute Differences ΔH_i

ΔH_1	ΔH_2	ΔH_3	ΔH_4	ΔH_5
69.8 N	68.8 N	68.7 N	67.8 N	67.6 N

5 CONCLUSION

The scope of this paper is the influence of the indentation rolling resistance on the energy requirement of a belt conveyor system. Due to the constantly increasing pressure to reduce CO₂, energy-optimized belts are considered essential in bulk material conveying technology. In addition, it explains how the indentation rolling resistance on the idlers occurs and thus dissipates energy. The development of new elastomer compounds, which need to be investigated, serves as levers here. To support the development of this multitude of possibilities, the ITA is working within an AiF-funded research project to support this development with simulations.

This paper shows that the measurement procedure according to DIN EN 16 974 is statistically suitable to validate belt models. For this purpose, the measurement procedure of four series of 24 measurements, with over all 120.000 values each, is investigated due to their standard deviation and normal distributions during the evaluation. It becomes clear that the indentation rolling resistance can be determined with high repeatability and at least low standard deviations ($S < 2$ N) from the scattering individual measured values using the evaluation procedure in conjunction with the measurement procedure. This leads to the conclusion that the determined indentation rolling resistances on the test rig are suitable for validating simulation models.

6 FUNDING REFERENCE

This publication was funded within the framework of the IGF project 20654 N ‘Energieoptimierte Auslegung von Förderanlagen durch Simulation des Eindrückrollwiderstandes (SimERW)’ by the ‘Forschungsgemeinschaft Intralogistik/Fördertechnik und Logistiksysteme (IFL) e.V.’ via the ‘Arbeitsgemeinschaft Industrieller Forschungsvereinigungen Otto von Guericke’ e.V. (AiF) within the framework of the program for ‘Förderung der Industriellen Gemeinschaftsforschung’ (IGF) funded by the ‘Bundesministerium für Wirtschaft und Energie’ (BMWi) based on a resolution of the Deutschen Bundestag.

LITERATURE

- [DAA18] VON DAAKE, S.: Berechnungsmodell zur Ermittlung des Eindrückrollwiderstandes von Schlauchgurtförderern. Dissertation Gottfried Wilhelm Leibniz Universität Hannover, 2018.
- [DIN11] DIN DEUTSCHES INSTITUT FÜR NORMUNG E.V.: DIN 22101 Stetigförderer – Gurtförderer für Schüttgüter – Grundlagen für die Berechnung und Auslegung. 12-2011.
- [DIN16] DIN DEUTSCHES INSTITUT FÜR NORMUNG E.V.: DIN EN 16974 Fördergurte – Gurtbreitenbezogener Eindrückrollwiderstand – Anforderungen, Prüfung. 11-2016.
- [GEE01] GEESMANN, F.-O.: Experimentelle und theoretische Untersuchungen der Bewegungswiderstände von Gurtförderanlagen. Dissertation Gottfried Wilhelm Leibniz Universität Hannover, 2001.
- [HIN93] HINTZ, A.: Einfluß des Gurtaufbaus auf den Energieverbrauch von Gurtförderanlagen. Dissertation Gottfried Wilhelm Leibniz Universität Hannover, 1993.
- [KÖN03] KÖNIG, J.: Modellierung des stationären Lauf eines Fördergurtes über eine Tragrollenstation. Dissertation Gottfried Wilhelm Leibniz Universität Hannover, 2003.
- [SCH04] SCHOLL, F.: Beitrag zur Bestimmung des Eindrückrollwiderstandes von Gurtförderanlagen. Dissertation Gottfried Wilhelm Leibniz Universität Hannover, 2004.
- [SCH66] SCHWARZ, F.: Untersuchungen zum Eindrückrollwiderstand zwischen Fördergurt und Tragrolle. Dissertation Technische Hochschule Hannover, 1966.
- [VIE60] VIERLING, O.: Grundlagen der Fördertechnik – Handschriftliche Mitschriften. Technische Hochschule Hannover, 1960, Hannover.
- [WEN08] WENNEKAMP, T.: Tribologische und rheologischen Eigenschaften von Fördergurten. Dissertation Gottfried Wilhelm Leibniz Universität Hannover, 2008.

Malte Kanus, M.Sc., Research Assistant at the Chair of Transport and Automation Technology, Leibniz University Hannover.

Malte Kanus was born 1990 in Hannover, Germany. Between 2010 and 2016, he studied mechatronic engineering at the Leibniz University Hannover.

Address: Institute of Transport and Automation Technology, Leibniz Universität Hannover, An der Universität 2, 30823 Garbsen, Germany

Phone: +49 511 762-18286, Fax: +49 511 762-4007, E-Mail: malte.kanus@ita.uni-hannover.de

Carsten Schmidt, M.Sc., Research Assistant at the Chair of Transport and Automation Technology, Leibniz University Hannover.

Carsten Schmidt was born 1993 in Willich, Germany. From 2012 to 2018, he passed the dual study program in corporation with AUMUND Fördertechnik GmbH and Rhein-Waal University of applied sciences in Kleve. Between 2018 and 2021, he studied mechanical engineering at the Leibniz University Hannover.

Address: Institute of Transport and Automation Technology, Leibniz Universität Hannover, An der Universität 2, 30823 Garbsen, Germany

Phone: +49 511 762-2547, Fax: +49 511 762-4007, E-Mail: carsten.schmidt@ita.uni-hannover.de

Prof. Dr.-Ing. Ludger Overmeyer, Head of the Institute of Transport and Automation Technology, Leibniz University Hannover.

Ludger Overmeyer was born 1964 in Recke, Germany. Between 1984 and 1991, he studied electrical engineering at the University of Hannover. In 1996 he finished his doctorate in mechanical engineering at the University of Hannover. From 1997 to 2001 he worked as project manager, division manager and head of research and development at Mühlbauer AG in Roding. Since 2001 Ludger Overmeyer is Professor at the Institute of Transport and Automation Technology of Leibniz University Hannover.

Address:
Institute of Transport and Automation Technology, Leibniz Universität Hannover, An der Universität 2, 30823 Garbsen, Germany

Phone: +49 511 762-3524, Fax: +49 511 762-4007, E-Mail: ludger.overmeyer@ita.uni-hannover.de